Progressive Change in Biomechanical Properties of Ex vivo Prostate with Pathology Fixation as Measured by MR Elastography at 7 Tesla, and Correlation with Changes in T_1, T_2 and ADC

D. M. McGrath[1], W. D. Foltz[1], and K. K. Brock[1,2]

[1]Radiation Medicine Program, Princess Margaret Hospital, Toronto, Ontario, Canada, [2]Department of Radiation Oncology, University of Toronto, Toronto, Ontario, Canada

INTRODUCTION There is increasing interest in the validation of medical imaging for disease detection and localization via correlation with the 'gold-standard' of histopathology (1). Whole-mount histology allows determination of the location and spatial extent of disease within an organ or tissue resection, and a 3D tissue volume can be reconstructed from the digitized slides (2), which contains the pathology-identified disease region as a sub-volume. To compare the disease locations identified by imaging and histology, the histopathology volume can be morphed into the in vivo imaging space using biomechanical registration (e.g., MORFEUS (3)). However, pathology processes, such as fixation in formalin solution, introduce further deformation. Hence, imaging of the whole ex vivo tissue specimen pre- and post-fixation is required to enable intermediate registration steps. Furthermore, fixation increases the tissue stiffness and measurements of these changes are required for biomechanical registration. Because the fixation period applied is variable between studies, it is informative to know how the effects vary over time. A quasi-static MR elastography (MRE) method at high field (7 tesla) has been applied to measure the progressive fixation-induced material property changes in ex vivo canine prostate as a function of fixation time. As T_1, T_2 and ADC have also been observed to decrease with fixation (4, 5) it was furthermore investigated if these parameters could provide surrogate markers of fixation-mediated material property changes. Finally, the same parameters were measured in clinical prostatectomy tissue pre- and post-fixation.

METHODS Between the preclinical and clinical portions of the study some imaging parameters were optimized for improved quality and more rapid acquisition, in line with time frames allowed by pathology for the clinical tissue. ***MRE:*** Each tissue sample was embedded in a cube (7×7×7 cm^3) of gel prior to imaging. The MRE compression device (6) consisted of a sample holder, a compression plate and mechanical piston, connected via an eccentric disk to a non-magnetic ultrasonic piezo-electric motor (USR60-E3N, Shinsei**,** Japan), providing compression at 1 Hz with maximum amplitude of 1.5 mm. The device was placed in the bore of a 7-T pre-clinical MRI scanner (70/30 BioSpec, Bruker, Ettlingen, Germany), where a quadrature volume resonator (15.5 cm inner diameter) was used for transmission and reception. Motion was tracked via the scanner preclinical respiration monitor (SA Instruments Inc., New York), which triggered the scanner to acquire during the compression phase. A Stimulated Echo (STEAM) sequence (6) was used, with gradient duration τ = 1 ms and amplitude Gd = 40 mT/m, implying a displacement sensitivity ϕ_d of 3.4π/mm. The mixing time T_m between the 2nd and 3rd STEAM 90° pulses was 200 ms, and TR was 1s. Acquisitions were made, while static and during motion, of 23 slices of 3 mm thickness, with 0.5 by 0.5 mm in-plane resolution (160 × 160 matrix) using echo planar (EPI) readout. ***T_1, T_2 and ADC:*** These parameters were quantified at consistent graphical prescription and voxel dimensions with the MRE acquisition. T_1 and T_2 were measured using a RARE (Rapid Acquisition with Relaxation Enhancement) method adapted for quantification using saturation recovery, over a range of echo times (7.5-112.5 ms) and repetition times (500-4000 ms), RARE factor = 2 and NEX=3. The diffusion experiment to measure ADC used EPI and 3 orthogonal gradient directions with b values = (0, 750 s/mm2) and Gd= 266 mT/m. ***Preclinical:*** A whole canine prostate specimen was obtained from a healthy adult dog (diameter ~3.5 cm). To observe the progressive effects of submersion in formalin (10% neutral buffered) the MRE, T_1, T_2 and ADC acquisitions were carried out while the sample was fresh and repeated after fixation over 12 h and further intervals of: 6 h (18 h total); 12 h (30 h total); 90 h (120 h total). The MRE EPI readout parameters were: TE = 18 ms; NEX = 12; segments = 10. At each time point the sample was embedded in gel before imaging and removed from gel for fixation. The ADC EPI parameters were TR = 3500 ms; TE = 27 ms; segments = 8; NEX=10. ***Clinical:*** A whole prostatectomy specimen (diameter ~ 4 cm) was received from a patient with biopsy-confirmed reoccurrence of cancer in the peripheral zone, after earlier treatment with targeted radiation therapy. The MRE, T_1, T_2 and ADC acquisitions were carried out while the sample was fresh and repeated after 60 h fixation. The MRE EPI readout parameters were: TE = 16 ms, NEX = 7, segments = 17. The ADC EPI readout parameters were: TR=4500 ms; TE= 23 ms; segments 17; NEX=4. ***Post-processing:*** Quantitative maps of Young's Modulus (*E*) were calculated for each MRE imaging slice using the methods outlined in (6). According to standard exponential functions, maps of T_1 and T_2 were generated using Bruker software (Paravision 5.0) and maps of ADC using Matlab (The MathWorks, Natick, MA). The tissue was manually segmented from the gel (Matlab) and the mean values for each parameter calculated.

RESULTS The parameter maps of the canine prostate in figure 1 show how fixation increases tissue stiffness (MRE *E*) progressively and non-uniformly with fixation, and as an approximate function of distance from the tissue edge. T_1 decreases with fixation and in an approximately uniform manner across the tissue. T_2 also decreases, but in a pattern that is more strongly a function of distance from the tissue edge. The margin of decrease in T_2 at 12 h is approximately 1 cm deep (red lines), and the margin depths at all time points correspond approximately to the predicted penetration depths for formalin (7, 8). ADC also decreases progressively, but in a less predictable pattern. Some areas of low ADC appear similar to areas of high MRE *E* (see arrows). Figure 2 demonstrates that while MRE *E* and T_2 change consistently with fixation time (2a and 2c), T_1 and ADC do not (2b and 2d), i.e., from 12 to 18 h fixation the mean values increase.

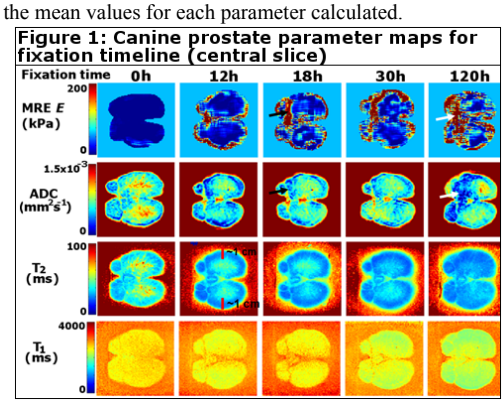

The maps of the clinical prostate sample in figure 3 demonstrate similar changes to the preclinical data for all parameters (*E*: 13-fold increase; T_1: -7%; T_2: -55%: ADC: -13%). Extra tissue excised with the prostate (dark in pre-fixation signal image) has low *E* values both pre- and post-fixation (i.e., consisted of highly porous tissue) and this was excluded when calculating the mean.

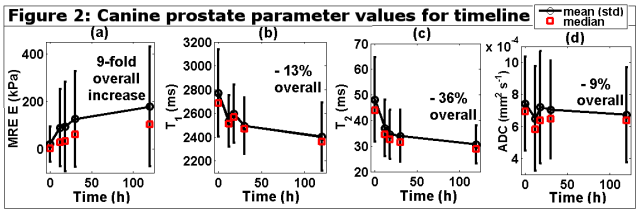

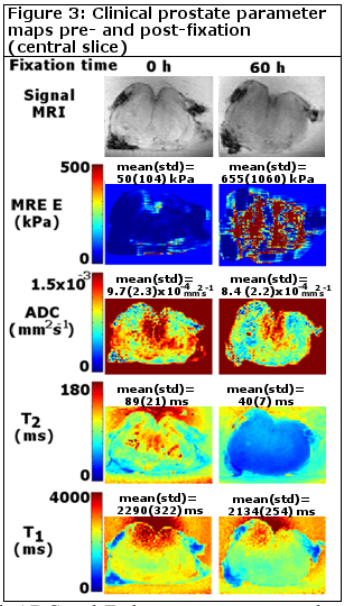

DISCUSSION AND CONCLUSION

In formalin T_1 and T_2 are thought to decrease predominantly by exchange of protons with formaldehyde (4). However, along with ADC and *E*, these parameters are also likely to be affected by the fixative-induced protein cross-linking (4). Furthermore, all the MRI parameters will be influenced by hydration, and repeated insertion and removal from solution for the timeline may have introduced secondary effects. As T_2 had a consistent response to formalin exposure (and greater than that of T_1 and ADC) it may allow prediction of increases in *E*. However, regional variations in ADC also appear to correlate with those of *E*, probably owing to a mutual high sensitivity to protein cross-linking. Further data will be collected from prostatectomy specimens to build population averages of all parameters. The MRE data will be used in the biomechanical registration of histology to imaging, and correlation of the MRE data with the other parameters should lead to models allowing prediction of material property changes, obviating the requirement for direct material property measurement of fresh and fixed ex vivo tissue.

REFERENCES 1. Breen MS et al, *Ann Biomed Eng* 2005, 33 (8), 1100-1112; 2. Clarke GM et al, *Histopathology* 2007,50,232-242; 3. Brock KK et al, *Med Phys* 2005,32:1647-1659; 4. Purea A et al, *Magn Reson Med* 2006,56:927-931; 5. Yong-Hing CJ et al, *Magn Reson Med* 2005 54:324–332; 6. McGrath DM et al, *Proc. ISMRM* 2010 p.640; 7. Medawar PB, *J R Microsc Soc* 1941;61:46-57; 8. Baker JR. *Principles of biological microtechnique: Metheun & Co.* Ltd; 1958 p.37-40.